Pramāṇa – J. Phys., Vol. 30, No. 5, May 1988, pp. 423–428. © Printed in India.

Lattice dynamics of $MgSiO_3$ perovskite

NARAYANI CHOUDHURY*, S L CHAPLOT, K R RAO and SUBRATA GHOSE†

Nuclear Physics Division, Bhabha Atomic Research Centre, Trombay, Bombay 400 085, India
† Mineral Physics Group, Department of Geological Sciences, University of Washington, Seattle, Washington 98195, USA

MS received 16 December 1987

Abstract. A lattice dynamical study of the geophysically important mineral $MgSiO_3$ in its orthorhombic perovskite phase, with space group Pnma (D_{2h}^{16}) has been carried out using a rigid ion model, with the potential consisting of Coulombic and short-ranged interactions. With the help of program DISPR, the ionic charges and radii were optimized using the equilibrium conditions. The resulting potential model is employed to predict the elastic constants and the phonon dispersion relations. The computed long wavelength optic modes are in good agreement with the corresponding experimental Raman and infrared active bands. The phonon density of states has been obtained and is used to evaluate the specific heat, the mean square displacements and thermal parameters of atoms.

Keywords. Lattice dynamics; $MgSiO_3$ perovskite; density of states; specific heat; thermal parameters.

PACS Nos 63·20; 65·40; 65·90

1. Introduction

The perovskite phases of $MgSiO_3$ and $CaSiO_3$ are generally accepted as the most abundant minerals in the earth's lower mantle (Reid and Ringwood 1975) and are believed to contribute to the seismic velocity discontinuities in the mantle at the depth of 650 km (Liu 1979). Despite its importance, useful experimental data of various physical properties under geophysically relevant conditions for $MgSiO_3$ perovskite are generally lacking. Theoretical predictions of the physical properties of this mineral and the variation in these properties with temperature and pressure have therefore aroused considerable interest. Computer simulations of the structure and elastic properties of $MgSiO_3$ perovskite have been reported by Wall *et al* (1986) and Matsui *et al* (1987). The study of relative stability of some of the possible perovskite polymorphs (Wall *et al* 1986) indicates that the orthorhombic phase is the most stable phase at all but the highest pressures (> 1·5 Mbar) where the cubic phase may be stable. X-ray diffraction measurements of the structure of polycrystalline $MgSiO_3$ perovskite at 1 Kbar (Yagi *et al* 1978) reveal that it is orthorhombic with space group Pnma. The theoretical study of lattice dynamics and equation of state of cubic perovskite type $MgSiO_3$ has been carried out by Hemley *et al* (1987); they find that the cubic structure of $MgSiO_3$ with space group Pm3m is dynamically unstable at all pressures, with

*To whom all correspondence should be addressed.

imaginary quasiharmonic phonons occurring at the edge of the Brillouin zone. To the best of our knowledge, no detailed lattice dynamical studies on orthorhombic $MgSiO_3$ perovskite have been reported earlier.

We have therefore undertaken a lattice dynamical study of the orthorhombic perovskite phase of $MgSiO_3$. The essential input for the calculations is a suitable potential function to represent the interatomic interactions. Our objective has been, (i) to obtain the static properties, viz the cohesive energy, and (b) to predict the dynamical properties, viz the elastic constants, the phonon dispersion relations, the phonon density of states and the specific heat as a function of temperature. In § 2, we discuss the structure of $MgSiO_3$ perovskite while § 3 outlines the lattice dynamical model used. In § 4, we discuss the computed phonon dispersion relation and density of states, while § 5 summarizes our results and conclusions.

2. Structure of $MgSiO_3$

The structure of perovskite type ABO_3 compounds is made up of a three-dimensional chain of BO_6 octahedra (Megaw 1972). In the ideal cubic perovskite (figure 1) the smaller cation (*B*) has a coordination number of six whereas the larger cation (*A*) is surrounded by twelve oxygen atoms. The distortion from the ideal cubic perovskite is caused by rotation and displacement of the octahedron structure. In orthorhombic perovskite the coordination of *B* is again six, but the number of oxygen atoms nearest to *A* varies with the degree of distortion. The crystal of $MgSiO_3$ perovskite is orthorhombic with space group Pnma (D_{2h}^{16}) (Ito and Matsui 1978; Yagi *et al* 1978). Its structure can be regarded as a three-dimensional network of corner sharing SiO_6 octahedra with magnesium ions occupying interstices among the octahedra. Each magnesium ion is surrounded by eight oxygen ions O(1) at distances less than 2·5 Å and four other oxygen ions O(2) at further distances between 2·8 and 3·2 Å. Both Mg and O(1) lie on mirror planes, Si at inversion centres and O(2) is in a general position. The lattice parameters and atomic positions for $MgSiO_3$ perovskite which has four formula units per unit cell are given in table 1.

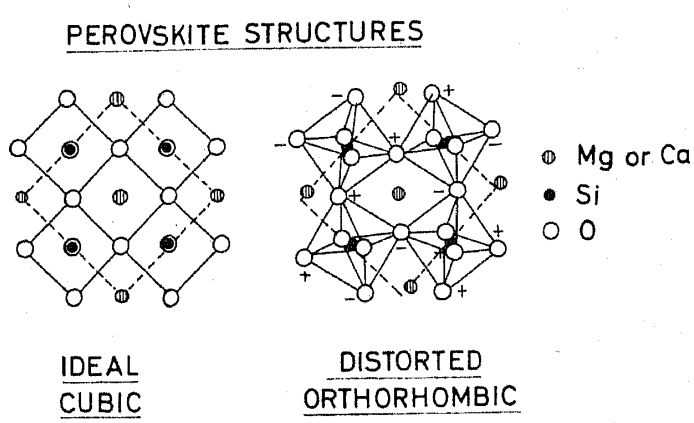

Figure 1. Ideal cubic and distorted perovskite structures (Megaw 1972).

Table 1. Lattice parameters and atomic positions (Yagi *et al* 1978). Space group: Pnma (D_{2h}^{16})

$a = 4{\cdot}933$ Å	$V = 162{\cdot}75$ Å^3
$b = 6{\cdot}902$ Å	$\rho = 4{\cdot}098$ gm/cc
$c = 4{\cdot}78$ Å	$Z = 4$ molecules/unit cell

	x	y	z
Mg	0·063(5)	0·25	0·974(7)
Si	0·5	0·0	0·0
O(1)	0·477(11)	0·25	0·096(10)
O(2)	0·291(7)	0·056(4)	0·696(7)

3. Lattice dynamical model

The lattice dynamical analysis is carried out assuming that the interactions among the constituents of the lattice can be described by an atom-atom potential function in the rigid ion model within the usual quasiharmonic approximation. The atom-atom potential function consists a long-ranged Coulomb interaction and a short-ranged Born-Mayer type repulsive interaction as in our earlier studies of other complex ionic crystals including silicates (Rao *et al* 1987). The potential energy between two non-bonded atoms k and k' separated by a distance r is given by

$$V(r) = (e^2/4\pi\varepsilon_0)\{[Z(k)Z(k')]/r\} + a\exp\left[\frac{-br}{R(k)+R(k')}\right] \tag{1}$$

with $a = 1822$ eV/atom, and $b = 12{\cdot}364$; and $Z(k)$ and $R(k)$ are respectively the charge and radii of the kth atom, and are treated as parameters. These parameters were evaluated using physicochemical considerations and equilibrium conditions that at equilibrium the forces on all the atoms must vanish and the system must be stressfree. The final parameters $Z(k)$ and $R(k)$ used are 1·5, 2·1 and $-1{\cdot}2$ for the charges and 1·43, 1·15, and 1·64 Å for the radii of Mg, Si and O atoms, respectively. The static lattice energy per unit cell was $-245{\cdot}67$ eV and the computed bulk modulus and elastic constants are given in table 2. The computed value of the bulk modulus at zero pressure (namely 247 GPa) is in excellent agreement with the corresponding experimental value of 247 GPa (Kudoh *et al* 1987). In table 2, we have also included the computed elastic constants of Matsui *et al* (1987) who obtain the structural and elastic properties of the perovskite phase of $MgSiO_3$ from a computational model based on energy minimization. Our elastic constants are systematically lower than those of Matsui *et al* (1987); but can be suitably scaled by varying the potential parameters.

4. Phonon dispersion relation and density of states

Group theoretical analysis of lattice vibrations of atomic crystals making use of irreducible multiplier representations has been carried out and the symmetry vectors of normal vibrations along the three high symmetry directions Σ, Δ, and Λ are derived.

Table 2. Elastic constants of $MgSiO_3$ perovskite in GPa.

	Present work (computed)	Matsui *et al* (1987) (computed)	Experimental Kudoh *et al* (1987)
K_0	243	261	247
C_{11}	367	506	
C_{22}	281	378	
C_{33}	323	460	
C_{44}	130	159	
C_{55}	77	112	
C_{66}	142	162	

These symmetry vectors have been used in block diagonalizing the dynamical matrix and the lattice dynamical model described above has been used to predict the phonon dispersion curves and their associated atomic motions, making use of program DISPR (Chaplot 1978). The phonon dispersion curves along the three directions are shown in figure 2. There are no degenerate modes along any of the three directions.

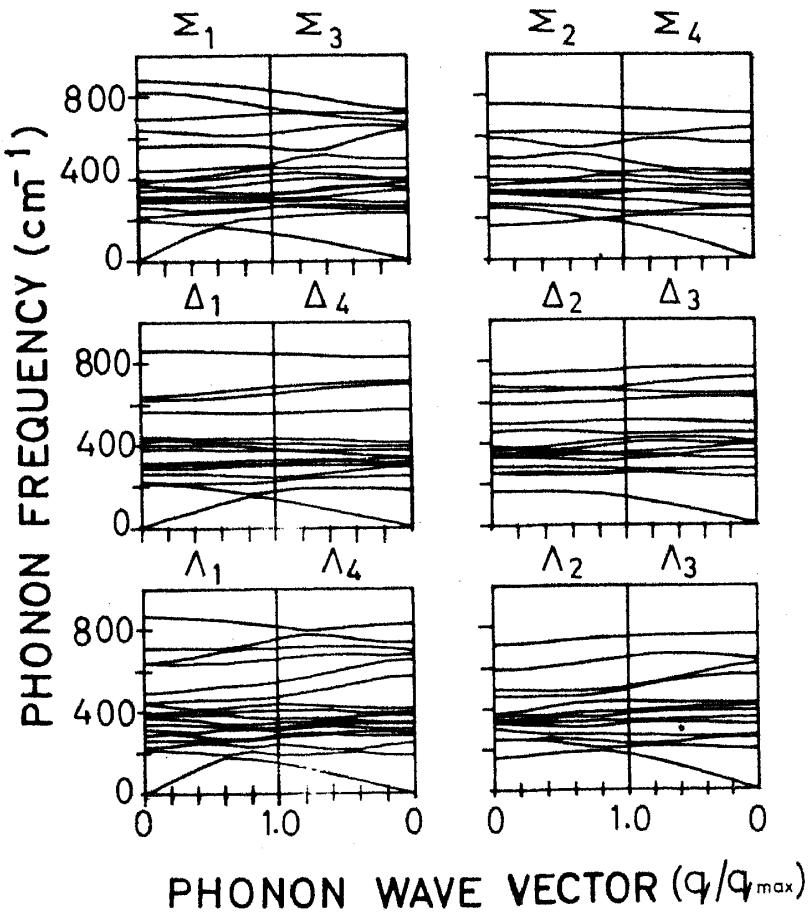

Figure 2. Phonon dispersion curves along the three high symmetry directions with wavevectors along **a*** (Σ), **b*** (Δ) and **c*** (Λ) directions. There are 60 phonon branches along each direction.

The density of states or frequency distribution of phonons is defined as

$$g(\omega) = A \int \sum_j \delta(\omega - \omega_j(\mathbf{q}))\, \mathrm{d}\mathbf{q},$$

where A is a normalization constant such that $\int g(\omega)\,\mathrm{d}\omega = 1$; and $\omega_j(\mathbf{q})$ is the phonon frequency of the jth normal mode of a phonon with wavevector $\mathbf{q}$. The root sampling method was used in obtaining $g(\omega)$ and the computed density of states is shown in figure 3. The density of states was used to evaluate the specific heat $C_v(T)$, given by,

$$C_v(T) = k \int \left(\frac{\hbar\omega}{kT}\right)^2 \frac{\exp(\hbar\omega/kT)}{[\exp(\hbar\omega/kT) - 1]^2} g(\omega)\,\mathrm{d}\omega,$$

where k is the Boltzmann constant and T is the temperature. The partial density of states $g_i^t(\omega)$ has been obtained as discussed in Choudhury *et al* (1986) and is used to evaluate the mean square displacements $\langle u_i^2 \rangle$ and thermal parameters B_i of atom i, given by,

$$\langle u_i^2 \rangle = C \frac{2\hbar}{m_i} \int \frac{\{(e^{\hbar\omega/kT} - 1)^{-1} + 1/2\}}{\omega} g_i^t(\omega)\,\mathrm{d}\omega$$

$$B_i = \frac{8\pi^2 \langle u_i^2 \rangle}{3}$$

where m_i is the mass of the ith atom, and C is a normalization constant normalizing $\langle u_i^2 \rangle$ to three degrees of freedom.

5. Results and conclusions

The density of states in figure 3 has peaks around 350 cm^{-1}, 550 cm^{-1}, and 700 cm^{-1} and has no band gaps as in forsterite (Rao *et al* 1987). The band gap in forsterite Mg_2SiO_4 was essentially due to the large difference between the vibrational frequencies corresponding to intermolecular and intramolecular vibrations of the silicate molecule;

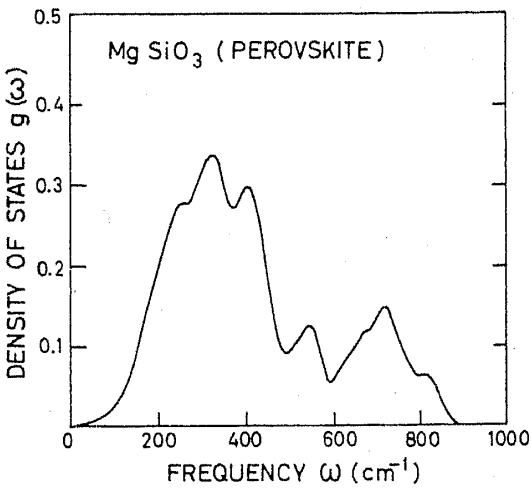

Figure 3. The computed density of states in the rigid-ion model.

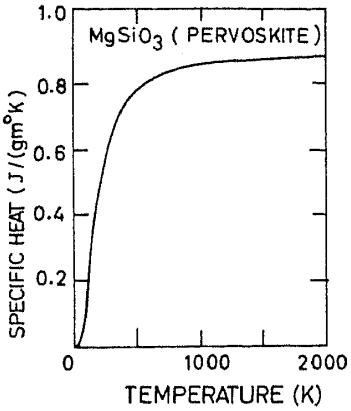

Figure 4. The computed specific heat as a function of temperature.

Table 3. Thermal parameters of atoms (Å^2).

	Mg	Si	01	02
Expt.^{A}	0·5	0·5	0·5	0·5
Exptl.^{B}	0·46	0·25	0·32	0·34
Calc.^{C}	0·516	0·408	0·432	0·432

A: Ito and Matsui (1978); *B*: Horiuchi *et al* (1987);
C: present work.

in $MgSiO_3$, however, SiO_3 is no longer a molecular unit and the density of states has no such band gaps. The specific heat as a function of temperature is shown in figure 4; to the best of our knowledge no experimental data on specific heat exist. The computed thermal parameters of atoms are compared with the experimental values in table 3 and the agreement is satisfactory. The range of the lowest and highest optic long wavelength modes ($\mathbf{q} \sim 0$) are in good agreement with the experimental values of Williams *et al* (1987) although no detailed mode by mode fitting has been attempted.

References

Chaplot S L 1978 *A computer program for external modes in complex ionic crystals (rigid molecular-ion model)*, BARC report 972
Choudhury N, Chaplot S L and Rao K R 1986 *Phys. Rev.* **B33** 8607
Hemley R J, Jackson M D and Gordon R G 1987 *Phys. Chem. Min.* **14** 2
Horiuchi H, Ito E and Weidner J 1987 *Am. Miner.* **72** 357
Ito E and Matsui Y 1978 *Earth Planet Sci. Lett.* **38** 443
Kudoh Y, Ito E and Takeda H 1987 *Phys. Chem. Min.* **14** 350
Liu L G 1979 *Geophys. Res. Lett.* **2** 417
Matsui M, Akaogi M and Matsumoto T 1987 *Phys. Chem.* Min. **14**
Megaw H 1972 *Crystal structures, A working approach* (Philadelphia: Samders)
Rao K R, Chaplot S L, Choudhury N, Ghose S and Price D L 1987 *Science* **236** 64
Reid A F and Ringwood A E 1975 *J. Geophys. Res.* **80** 3363
Wall A, Price G D and Parker S C 1986 *Min. Mag.* **50** 693
Williams Q, Jeanloz R and McMillan P 1987 *J. Geophys. Res.* **B92** 8116
Yagi T, Kwang M H and Bell P M 1978 *Phys. Chem. Min.* **3** 97